# Au-NHC@Porous Organic Polymers: Synthetic Control and Its Catalytic Application in Alkyne Hydration Reactions

Wenlong Wang,[†,‡] Anmin Zheng,[§] Peiqing Zhao,[†] Chungu Xia,[†] and Fuwei Li*[†,∥]

[†]State Key Laboratory for Oxo Synthesis and Selective Oxidation, Lanzhou Institute of Chemical Physics, Chinese Academy of Sciences, Lanzhou, Gansu 730000, P. R. China

[‡]University of the Chinese Academy of Sciences, Beijing, P. R. China

[§]State Key Laboratory of Magnetic Resonance and Atomic and Molecular Physics, Wuhan Center for Magnetic Resonance, Wuhan Institute of Physics and Mathematics, Chinese Academy of Sciences, Wuhan 430071, China

[∥]Suzhou Institute of Nano-Tech and Nano-Bionics, Chinese Academy of Sciences, Suzhou 215123, China

Ⓢ *Supporting Information*

**ABSTRACT:** The synthetic control and functions of porous organic polymers (POPs) with N-heterocyclic carbene gold(I) (Au-NHC@POPs) are described in this article. A series of Au-NHC@POPs with tunable physical properties such as surface area and pore size distribution were first synthesized via Sonogashira chemistry by differing monomer strut lengths and concentration during polymerization; a controllable transition from nonporous to microporous and the coexistence of micro- and mesoporous structures in the framework were realized by varying the monomer concentration. To explain this phenomenon, we put forward a model assumption of a branch−branch cross effect. Additionally, Au-NHC@POPs1 was found to have superior catalytic activity in alkyne hydration reactions, and the catalyst could be used six times with a slight loss of activity.



**KEYWORDS:** *N-heterocyclic carbene, porous organic polymers, synthetic control, alkyne hydration, cross-coupling*
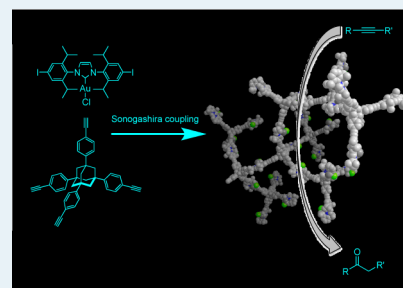
## 1. INTRODUCTION

Homogeneous catalysts, especially organometallic catalysts, play an extremely important role in the field of modern catalysis. However, most precious organometallic catalysts have not been widely used because of their complicated synthesis, intricate recycling problem, and thus the metal contamination of the products.[1,2]

So far, the main method of recycling organometallic complexes is to heterogenize the homogeneous catalysts, for instance, the classical anchoring method, in which the catalyst is anchored to various kinds of supports, such as silica-based materials[3−7] and magnetic nanoparticles.[8−10] However, the catalytic moieties are inhomogeneously distributed and pendent into the pore volume, which may cause pore blocking and eventually deactivate the catalytic system.[11] Recently, porous organic materials, including porous organic polymers (POPs),[12−20] metal−organic frameworks (MOFs),[21,22] and covalent organic frameworks (COFs)[23−25] have emerged as a versatile platform for the deployment of catalysts because of its porous nature and high surface area. Nonetheless, it should be noted that MOFs and COFs are unstable in many circumstances such as acid, base, and moisture because of the whole MOFs' connection of coordination bonds and the presence of boronate ester or imine groups in COFs, which severely limit their applications in catalysis. In contrast, POPs are advantageous compared to MOFs and COFs in terms of hydrothermal stability and chemical robustness.

Catalytic POPs could be divided into two major classes: POPs that are incorporated uniformly and covalently built-in homogeneous catalysts as building blocks and POPs that can be modified by postsynthesis[26−31] (generally, catalysts are loaded via noncovalent interactions). The first class has more flexibility in building block design, higher thermal and chemical stability due to the diversity of the organometallic catalysts, and all the linkage of covalent bonds. For example, Lin et al. developed the synthesis of bpy-ligated, Ir- and Ru-incorporating porous cross-linked polymers (PCPs) for efficient photocatalysis using $Co_2(CO)_8$-catalyzed alkyne trimerization.[32] Cooper's group elaborated the synthesis of bpy-ligated complex-functionalized conjugated microporous polymers (CMPs) via Sonogashira chemistry as an efficient heterogeneous catalyst for reductive amination.[33] Jiang and co-workers reported the direct synthesis and catalytic application of CMP-type iron porphyrin networks via Suzuki−Miyaura coupling chemistry.[34] For other catalytic POPs, see refs 35−39.

As for most of the reported active catalytic building blocks described above, metal elements are coordinated with neutral nitrogen ligands in a relatively unstable way. Recently, N-heterocyclic carbenes (NHCs) have emerged as excellent ligands with strong σ-electron donation ability, and their

coordination complexes with transition metals have found outstanding applications in homogeneous catalysis.[40−42] Nevertheless, most of them are synthesized through multiple steps and can be used only one time in homogeneous catalysis. Therefore, covalently built-in catalytic POPs based on NHC complexes have great potential, and their development for sustainable catalysis is highly desirable.

In addition, Cooper's work reported that physical properties such as micropore size and surface area of CMPs could be finely tuned by varying the monomer strut length,[43] and some earlier works reported the use of different solvents to influence porosity.[44,45] It is well-known that large surface areas and a suitable pore size distribution of the porous catalyst play a key role in its catalytic activity. With our continuing studies of the development of recyclable metal-NHC catalysts,[46,47] herein, we report the direct controllable synthesis of catalytic POPs (Au-NHC@POPs) with tunable physical properties based on an N-heterocyclic carbene gold(I) complex as building block via Sonogashira coupling by varying the monomer strut length and concentration during polymerization (Scheme 1).

**Scheme 1. (a) Synthesis of Au-NHC@POPs Using the Pd-Catalyzed Sonogashira Coupling Method and (b) Synthesis of NHC-salt@POPs**
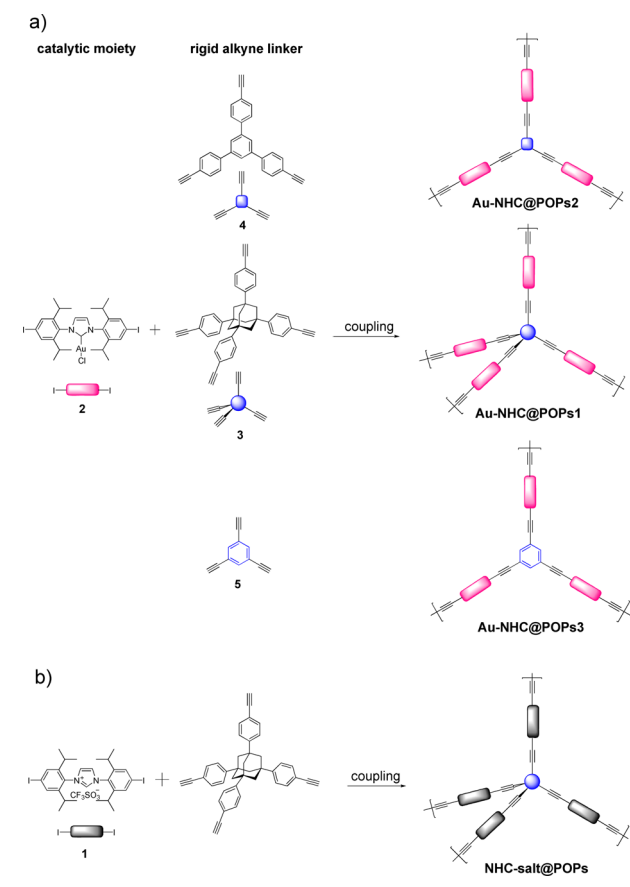


## 2. EXPERIMENTAL SECTION

**2.1. Synthesis of N-Heterocyclic Carbene Gold(I) Building Block and Alkyne Monomers.** The synthetic route of N-heterocyclic carbene gold(I) building blocks (**2**) is shown in Scheme 2. Iodine-functionalized [IPr]·HSO$_3$CF$_3$ (**1**) was synthesized according to the previously reported procedure

**Scheme 2. Synthesis of Iodine-Functionalized [(IPr)AuCl] Building Blocks**
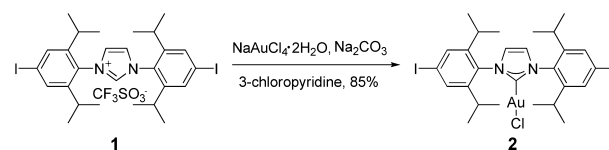


of Yang et al.[4] Iodine-functionalized [(IPr)AuCl] could be prepared in 85% yield in 3-chloropyridine by the reaction of NaAuCl$_4$·2H$_2$O with imidazolium salt and base (Na$_2$CO$_3$ or K$_2$CO$_3$).[48−50] Au-NHC coordination was established with the absence of the $^1$H resonance NCHN proton of precursor **1**. All the alkyne monomers were synthesized according to reported procedures.[51,52]

**2.2. Synthesis of Au-NHC@POPs and NHC-salt@POPs.** The synthetic schemes of Au-NHC@POPs and NHC-salt@POPs are shown in Scheme 1. To tune the physical properties of Au-NHC@POPs, alkyne monomers with different lengths were selected as linkers. Iodine-functionalized building block [(IPr)AuCl] **2** (0.24 mmol) was polycondensed with alkyne monomers **3** (0.12 mmol), **4** (0.16 mmol), and **5** (0.16 mmol) under the condition of the same catalyst loading and solvent amount (150 mL of toluene) via the Pd-catalyzed Sonogashira coupling strategy to form Au-NHC@POPs. NHC-salt@POPs were synthesized from [(IPr)HCF$_3$SO$_3$] **1** (0.24 mmol) and monomer **3** (0.12 mmol) under the same conditions that were used for Au-NHC@POPs (for detailed experiments, see the Supporting Information).

## 3. RESULTS AND DISCUSSION

**3.1. Characterization of the Material.** N$_2$ adsorption and desorption isotherms of Au-NHC@POPs and NHC-salt@POPs are shown in Figure 1. Compared with Au-NHC@
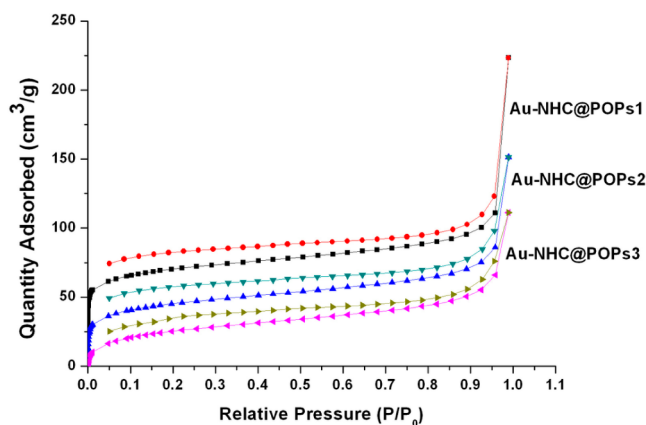


**Figure 1.** N$_2$ adsorption−desorption isotherm measured at 77 K.

POPs2 ($S_{BET}$ = 350 m$^2$/g) and Au-NHC@POPs3 ($S_{BET}$ = 258 m$^2$/g), Au-NHC@POPs1 with monomer **3** as a linker has the maximal surface area ($S_{BET}$ = 506 m$^2$/g). This is mainly due to the larger monomer with its four alkyne groups stretching to four sides in a tetrahedral way that is different from that of monomers **4** and **5** that stretched in a plane triangular way. In addition, the surface area of NHC-salt@POPs ($S_{BET}$ = 249 m$^2$/g) is much smaller than that of Au-NHC@POPs1; this is possibly because of the pore blocking of the CF$_3$SO$_3$$^−$ anion. Nitrogen sorption of Au-NHC@POPs1 displayed a combina-

tion of type I and type II sorption isotherm curves along with a large adsorption at low pressure ($P/P_0 < 0.1$), which is suggestive of the coexistence of micro- and mesopores in the framework (for relative pore size distribution curves, see Figure S2 of the Supporting Information).

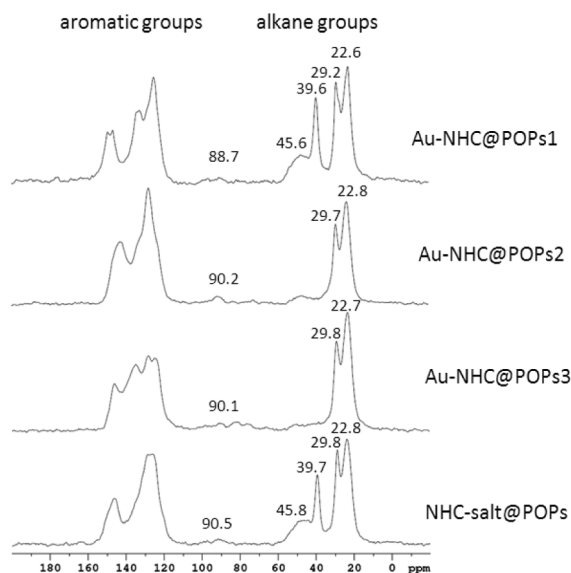Solid-state $^{13}$C NMR spectra (Figure 2) were measured to confirm the structures of Au-NHC@POPs and NHC-salt@



**Figure 2.** Solid-state NMR spectra of Au-NHC@POPs and NHC-salt@POPs.

POPs. The peaks at ∼22 and ∼29 ppm correspond to the carbon atom of the -CH$_3$ group and the tertiary carbon atom of the -CH(CH$_3$)$_2$ group, respectively. The signals at ∼39 and ∼45 ppm are ascribed to the secondary carbon (-CH$_2$) and the quaternary carbon atom connected with the phenyl group (Ar-C) of adamantane. The peak at ∼90 ppm is ascribed to sp-hybridized -Car-C≡C-Car- sites. The peaks between 120 and 160 ppm are confirmed to be aromatic groups.

Bond formation was further confirmed by the FT-IR comparison of monomer **2**, monomer **3**, Au-NHC@POPs1, Au-NHC@POPs2, Au-NHC@POPs3, and NHC-salt@POPs (Figure 3). In the spectra of Au-NHC@POPs and NHC-salt@POPs, the ≡C−H stretch and Ar−I stretch are diminished to
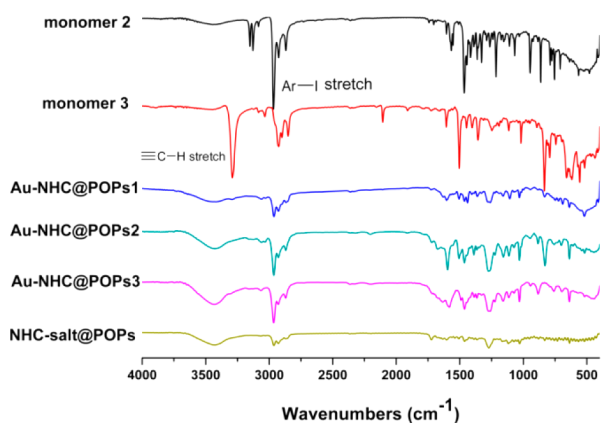


**Figure 3.** FT-IR comparison of monomer **2**, monomer **3**, Au-NHC@POPs1, Au-NHC@POPs2, Au-NHC@POPs3, and NHC-salt@POPs.

undetected levels, suggesting the bond formation of Sonogashira coupling. The high degree of spectral similarity of the four POPs also demonstrates the structural consistency of these materials.

To further study the valence-state information of the Au-NHC monomer in Au-NHC@POPs, characterization of the X-ray photoelectron spectra (XPS) was employed to investigate the variations of binding energy (BE) of Au between monomer **2** and Au-NHC@POPs. As shown in Figure 4, all the Au 4f$_{7/2}$
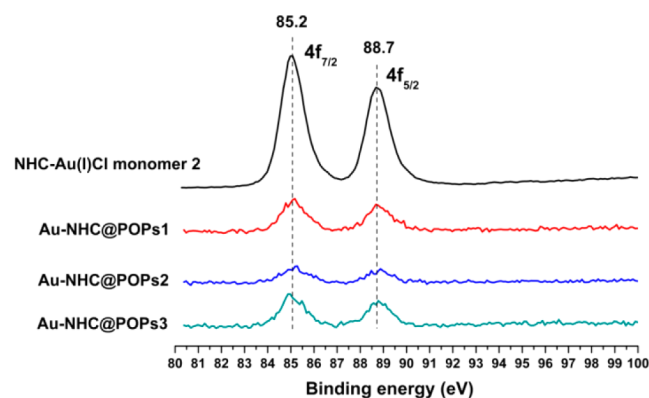


**Figure 4.** XPS comparison of NHC-Au(I)Cl monomer **2**, Au-NHC@POPs1, Au-NHC@POPs2, and Au-NHC@POPs3.

and 4f$_{5/2}$ peaks correspond well at 85.2 and 88.7 eV, respectively, which strongly confirmed the well-retained state of Au-NHC monomers **2** in Au-NHC@POPs. The Au-NHC monomers were successfully doped into these POPs.

The composition of these POPs was determined by combustion elemental analysis (EA for C, H, and N) and atomic absorption spectroscopy (AAS for Au). All experimental values (wt %; C 60.36, H 4.18, N 2.97, Au 18.45 for Au-NHC@POPs1; C 60.12, H 4.09, N 3.01, Au 18.51 for Au-NHC@POPs2; C 55.63, H 4.11, N 3.26, Au 21.42 for Au-NHC@POPs3; and C 66.87, H 5.14, N 3.09 for NHC-salt@POPs) are lower in comparison to the values calculated for an ideal structure assuming a 100% cross-linking degree (wt %; C 64.82, H 5.89, N 3.15, Au 22.15 for Au-NHC@POPs1; C 64.64, H 5.54, N 3.21, Au 22.55 for Au-NHC@POPs2; C 58.29, H 5.59, N 3.88, Au 27.31 for Au-NHC@POPs3; and C 72.93, H 6.62, N 3.47). This difference might be attributed to the residual functional groups (I). Interestingly, the N/Au molar ratios were >2. We found it because of the small part of insoluble catalysts in nitromurlatic acid during the normal AAS sample preparation. If the samples were treated with a high temperature of 600 °C in the muffle furnace, then the samples could be dissolved completely in the nitromurlatic acid. Surprisingly, the reprepared AAS sample provided a higher Au content (for details, see the Supporting Information). In addition, thermogravimetric (TG) analysis showed all these materials have thermal stability up to 300 °C (Figure S4 of the Supporting Information).

## 3.2. Synthesis and Characterization of Au-NHC@POPs1 in Different Amounts of Solvent Systems.
In addition, X-ray powder diffraction analysis of Au-NHC@POPs1 revealed no diffraction, implying that these POPs are amorphous (Figure S3 of the Supporting Information). As we know, the condensation reaction of COFs occurs in a reversible and dynamic fashion.[24,53] The chemical bonds of the forming polymers have to close and open to yield the thermodynami-

cally stable yet crystalline structures. However, the condensation process of POPs takes place in an irreversible way, which is totally different from that of COFs. Therefore, the idea of kinetic control in the synthesis of POPs naturally came to mind. In this work, the kinetically synthetic control of POPs was realized by varying the monomer concentration. Monomer **2** (0.24 mmol) and monomer **3** (0.12 mmol) were polycondensed under the same catalyst loading conditions but with different amounts of solvent (50, 80, 100, 120, and 150 mL of toluene) (for detailed experiments, see the Supporting Information). To our delight, a controllable transition from nonporous to microporous and the coexistence of micro- and mesoporous structures in the framework were found (for N2 adsorption and desorption isotherms, see Figure 5). Corre-
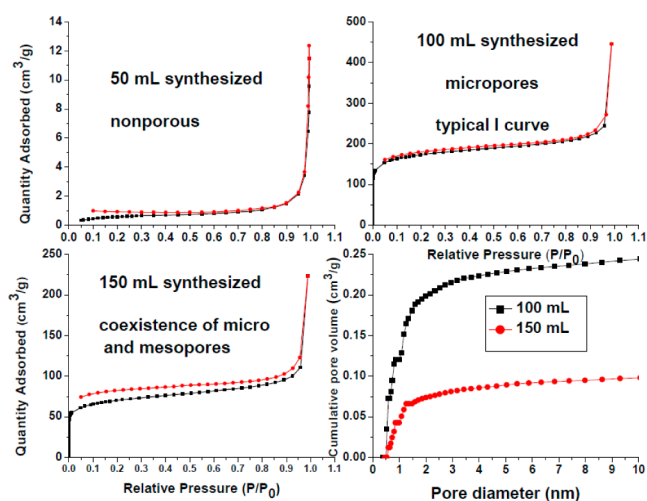


**Figure 5.** N2 adsorption−desorption isotherm of Au-NHC@POPs1 prepared different amounts of solvent systems measured at 77 K and pore size distribution calculated by NLDFT of Au-NHC@POPs1 prepared in 150 and 100 mL of toluene.

spondingly, the BET surface areas increased gradually from a very low point ($S_{BET}$ = 16 m²/g) to a peak value ($S_{BET}$ = 798 m²/g) and then decreased to a medium value ($S_{BET}$ = 506 m²/g) (Figure 6). This is possibly due to the pore blocking caused by the high reaction rate at high concentrations. To explain the concentration-controlled synthesis of Au-NHC@POPs, a model assumption of the branch−branch cross effect was proposed as shown in Figure S5 of the Supporting Information. When the polycondesation occurs in a 50 mL toluene system,
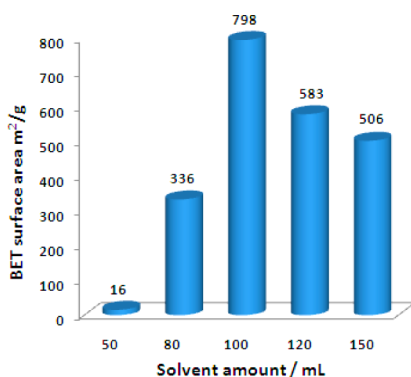


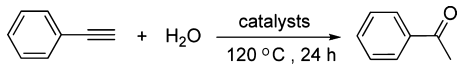**Figure 6.** Changes in BET surface areas (Au-NHC@POPs1) in different amounts of solvent.

the reaction rate was too fast (for time-dependent experimental results, see Figure S1 of the Supporting Information) and caused complete pore blocking by the branch−branch cross effect (Figure S5 of the Supporting Information).

Nevertheless, with the gradually reduced concentration, the reaction rate decreased and the branch−branch cross effect weakened gradually. When the pore blocking reaches a certain degree (in a 100 mL solvent system), microporous POPs with the highest surface area ($S_{BET}$ = 798 m²/g) were prepared. Finally, POPs ($S_{BET}$ = 506 m²/g) with the coexistence of micro- and mesoporous structures in the framework were synthesized in a 150 mL solvent system when the branch−branch cross effect decreased to a much lower degree.

It is worth noticing that the Au content and other element contents in each sample synthesized in different amounts of solvent were very similar (wt %; C 60.36, H 4.18, N 2.97, Au 18.45 for Au-NHC@POPs1 synthesized in 150 mL; C 60.38, H 4.17, N 2.96, Au 18.42 for Au-NHC@POPs1 synthesized in 120 mL; C 60.35, H 4.18, N 2.95, Au 18.43 for Au-NHC@POPs1 synthesized in 100 mL; C 60.37, H 4.15, N 2.97, Au 18.48 for Au-NHC@POPs1 synthesized in 80 mL; and C 60.34, H 4.17, N 2.97, Au 18.49 for Au-NHC@POPs1 synthesized in 50 mL).

**3.3. Alkyne Hydration Reactions Catalyzed by Au-NHC@POPs.** Alkyne hydration reactions have gained prime interest because of the wide availability of alkyne substrates and the fundamental importance of the carbonyl motif in organic synthesis.[54] Recently, Nolan and co-workers reported their (NHC)Au/AgSbF6 catalytic system that is the most efficient homogeneous system ever reported for an alkyne hydration reaction.[55] In this account, we also wish to investigate our newly synthesized Au-NHC@POPs as a sort of efficient, recoverable, and reusable heterogeneous catalyst in alkyne hydration reactions.

To begin, we explored this possibility of using phenylacetylene as the substrate in a heterogeneous system. Phenylacetylene (1 mmol) and Au-NHC@POPs1 (5 mg, equivalent to 5.62 μmol of Au) as a catalyst together with AgSbF6 (5 mg) as cocatalyst were refluxed at 120 °C in a sealing tube loaded with H2O (330 μL) and CH3OH (660 μL) for 24 h. As a result, the corresponding acetophenone was obtained in 86% yield. It is worth mentioning that in pure water, no product was observed, which implies that methanol is not innocent in this reaction; this is possibly due to the hydrophobicity of these materials and the fact that the pore structure is not wetted without the addition of methanol.[56] For comparison, we then investigated other POPs as catalysts, and Table 1 summarizes the catalytic performances of different catalysts. Besides the acetophenone, no other products were identified, suggesting all these catalysts were exclusively selective. NHC-salt@POPs were inactive, which implied that the Au active sites were essential for the present reactions or there is an ion exchange between SbF6− and CF3SO3−. However, when AgSbF6 was removed from the catalyst system, no product was observed. Therefore, these results clearly demonstrate that the alkyne hydration could not be realized without the assistance of AgSbF6. Au-NHC@POPs1 (86, 85, 86, and 73% yield for POPs prepared in different amounts of solvent), Au-NHC@POPs2 (83%), and Au-NHC@POPs3 (75%) all exhibited >70% yields of the desired aryl ketone except for nonporous Au-NHC@POPs1 (<10%, synthesized in 50 mL of toluene). This is possibly due to the small size of phenylacetylene [0.76 nm (see Figure S6 of the Supporting

**Table 1. Catalytic Performances of Different Catalyst Systems**[a]



| sample | $S_{BET}$ $(m^2/g)$ | $CH_3OH$ $(\mu L)$ | $AgSbF_6$ (mg) | yield[b] (%) |
|---|---|---|---|---|
| Au-NHC@POPs1[c] | 506 | 660 | 5 | 86 |
| Au-NHC@POPs1[c] | 506 | 660 | 0 | 0 |
| Au-NHC@POPs1[c] | 506 | 0 | 5 | trace |
| Au-NHC@POPs1[d] | 336 | 660 | 5 | 73 |
| Au-NHC@POPs1[e] | 798 | 660 | 5 | 86 |
| Au-NHC@POPs1[f] | 583 | 660 | 5 | 85 |
| Au-NHC@POPs1[g] | 16 | 660 | 5 | trace |
| Au-NHC@POPs2 | 350 | 660 | 5 | 83 |
| Au-NHC@POPs3 | 258 | 660 | 5 | 75 |
| NHC-salt@POPs | 249 | 660 | 5 | 0 |
| iodo-NHC-Au(I) | – | 660 | 5 | 88 |

[a]Reaction conditions: phenylacetylene (1 mmol), $H_2O$ (330 $\mu L$). [b]Isolated yield. [c]Au-NHC@POPs1 synthesized in 150 mL of toluene. [d]Au-NHC@POPs1 synthesized in 80 mL of toluene. [e]Au-NHC@POPs1 synthesized in 100 mL of toluene. [f]Au-NHC@POPs1 synthesized in 120 mL of toluene. [g]Au-NHC@POPs1 synthesized in 50 mL of toluene.

Information)] that can pass in and out freely in those micropores of the Au-NHC@POPs; therefore, no obvious catalytic difference was observed among these porous catalysts. To improve our understanding of the catalytic efficiency of Au-NHC@POPs1 synthesized in different amounts of solvent, kinetic studies of these catalysts were performed; a plot of the GC yield versus reaction time and the TOF value of the initial 2 h are shown in Figure 7, and we can conclude that Au-NHC@
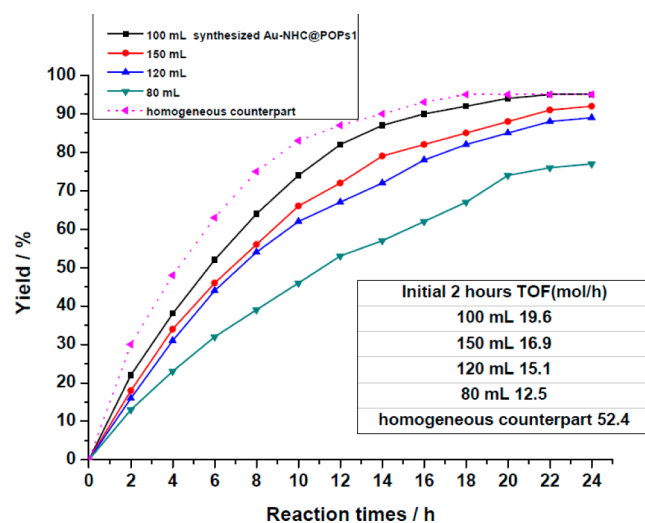


**Figure 7.** Plot of yield (GC yield) vs reaction time and the TOF (moles per hour) of the initial 2 h.

POPs1 synthesized in 100 mL had the best catalytic efficiecy (initial 2 h TOF, 19.6 mol/h) and its analogues synthesized in 80 mL had the worst catalytic result with a 12.5 mol/h of the initial 2 h TOF. Therefore, the morphology (surface areas and pore size distrbution) of the Au-NHC@POPs1 played an important role and had an impact on the early state of the reactions. In addition, the catalytic activity of the homogeneous counterpart (iodo-NHC-Au) was tested as a comparison with the newly synthesized heterogeneous catalyst, which exhibited a yield (88%) close to that of Au-NHC@POPs1.

To further elucidate the substrate size effect, a larger molecule [7**j** (Table 2)] up to 2.11 nm (see Figure S6 of the

**Table 2. Au-NHC@POPs1-Catalyzed Alkyne Hydration Reactions**[a]
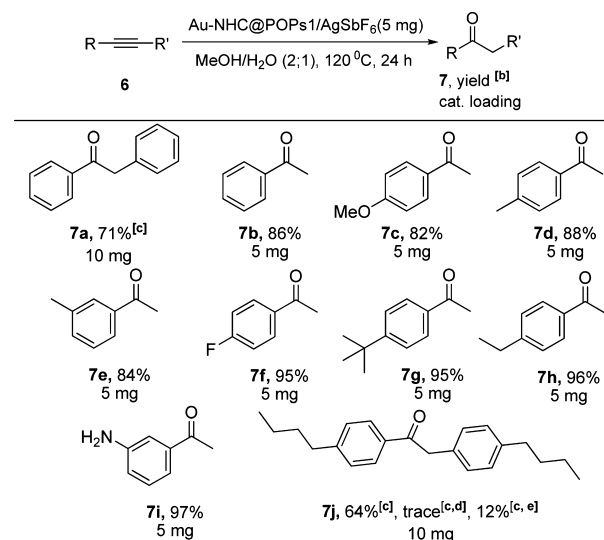


[a]Reaction conditions: **6** (1.0 mmol), Au-NHC@POPs1 (synthesized in 150 mL of toluene), MeOH (660 $\mu L$), $H_2O$ (330 $\mu L$). [b]Isolated yield. [c]1,4-Dioxane instead of MeOH. [d]Au-NHC@POPs1 synthesized in 50, 80, and 120 mL of toluene. [e]Au-NHC@POPs1 synthesized in 100 mL of toluene.

Supporting Information) was synthesized to test these different catalysts (Au-NHC@POPs1 that were prepared in 150, 120, 100, 80, and 50 mL of toluene). An interesting observation is the fact that 7**j** affords a 64% yield catalyzed by Au-NHC@POPs1, which was prepared in 150 mL of toluene, but only a trace or little (12%) product was detected when the reaction was catalyzed by Au-NHC@POPs1, which was synthesized in 50, 80, 120, and 100 mL of toluene. This is most likely because of the 2.11 nm large molecule that cannot pass through micropore networks freely. However, Au-NHC@POPs1 prepared in 150 mL of toluene exhibits the coexistence of micropores and mesopores that have a capacity for large molecules. All the experiments described above demonstrated that the pore size effect severely impacts catalytic efficiency. Subsequently, we examined the scope of this catalytic system. As shown in Table 2, the reactivity of terminal alkynes is better than that of internal alkynes. Substrates with electron-donating or electron-withdrawing groups all afforded good yields.

A favorable feature of the catalytic system that caught our attention was the precipitation of Au-NHC@POPs from the reaction mixture. Thus, we investigated the possibility of recycling Au-NHC@POPs. The catalyst was collected by centrifugation and then reused for the next round of alkyne hydration. Because of the high thermal stability and exceptional chemical robustness, Au-NHC@POPs1 was reused five times with only a slight loss of activity (Figure 8a). To better test the stability of catalyst Au-NHC@POPs1, a recycling experiment was conducted by increasing the level of the alkyne substrate to 3.0 mmol with 5 mg of Au-NHC@POPs1 to achieve an ~30% yield of acetophenone (Figure 8, b). Recycling the catalyst Au-NHC@POPs1 over five runs did not lead to a significant
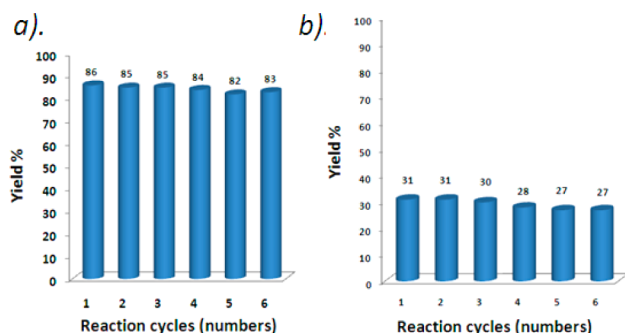
**Figure 8.** Recyclability test of Au-NHC@POPs1 in the model of phenylacetylene hydration: (a) 1 mmol of alkyne substrate and (b) 3 mmol of alkyne substrate.

decline in acetophenone yields. Analysis of the aqueous reaction solution after each cycle by ICP-AES showed Au element leaching did not reach the detection limit of 1 mg/L. Moreover, when the recycling experiment had been completed, the filtrate was used solely as the reaction medium without adding the heterogeneous Au-NHC@POPs1, and then the substrates were added to the reaction system to continue the reaction. The result showed that the GC yield of acetophenone was almost constant, which ensured the heterogeneous nature of the catalytic process.

It is worth noting that the IR spectral measurement of Au-NHC@POPs1 after reaction with pure water or a combination of water and methanol (1:2 volume ratio) produced almost the same spectrum of fresh Au-NHC@POPs1; no carbonyl group, which is generated from the hydration of the alkyne skeleton of this POPs catalyst, was observed (see Figures S7 and S8 of the Supporting Information). This is additional strong evidence of the hydrothermal stability of Au-NHC@POPs and Au elements that could not be easily separated from the POPs. Moreover, it is possible because of the structural rigidity of the framework that the Au sites cannot easily reach the alkyne groups of the Au-NHC@POPs. In addition, XPS characterization of Au-NHC@POPs1 after catalytic runs showed the well-retained state of Au-NHC catalytic species (Figure S9 of the Supporting Information).

## 4. CONCLUSION

In summary, for the first time, we have successfully prepared a series of catalytic POPs materials (Au-NHC@POPs) with the Au-NHC complex as building-in feedstock; their surface areas and pore size distribution can be tuned not only by the monomer structure but also through concentration control, and a model assumption of the branch−branch cross effect was proposed to explain the synthetic control. These Au-NHC@POPs have been found to be efficient heterogeneous catalysts for alkyne hydration reactions with good substrate tolerance and could be reused at least five times without a significant loss of catalytic efficiency. Control experiments with the larger alkyne proved the pore sized effect could severely impact the catalytic activity of a specific molecule. In addition, Au-NHC@POPs have good hydrothermal stability. These unique characteristics clearly indicate that POP catalysts based on covalently and homogeneously active metal-NHC sites could provide new potential in the exploration of built-in heterogeneous catalysts and their applications in sustainable catalyses.

## ■ ASSOCIATED CONTENT

**ⓢ Supporting Information**
Experimental details and characterizations of all compounds, TGA, IR, and pore size distribution profile. This material is available free of charge via the Internet at http://pubs.acs.org.

## ■ AUTHOR INFORMATION

**Corresponding Author**
*E-mail: fuweili@licp.cas.cn.

**Notes**
The authors declare no competing financial interest.

## ■ ACKNOWLEDGMENTS

## ■ REFERENCES

(1) Cole-Hamilton, D. J. *Science* **2003**, *299*, 1702.
(2) Robinson, A. L. *Science* **1976**, *194*, 1261.
(3) Zhu, F. X.; Wang, W.; Li, H. X. *J. Am. Chem. Soc.* **2011**, *133*, 11632.
(4) Zhou, H.; Wang, Y. M.; Zhang, W. Z.; Qu, J. P.; Lu, X. B. *Green Chem.* **2011**, *13*, 644.
(5) Yang, H. Q.; Li, G.; Ma, Z. C.; Chao, J. B.; Guo, Z. Q. *J. Catal.* **2010**, *276*, 123.
(6) Allen, D. P.; Wingerden, M. M. V.; Grubbs, R. H. *Org. Lett.* **2009**, *11*, 1261.
(7) Qiu, H.; Sarkar, S. M.; Lee, D. H.; Jin, M. J. *Green Chem.* **2008**, *10*, 37.
(8) Yang, H.; Wang, Y.; Qin, Y.; Chong, Y.; Yang, Q.; Li, G.; Zhang, L.; Li, W. *Green Chem.* **2011**, *13*, 1352.
(9) Wittmann, S.; Schätz, A.; Grass, R. N.; Stark, W. J.; Reiser, O. *Angew. Chem., Int. Ed.* **2010**, *49*, 1867.
(10) Ranganath, K. V. S.; Kloesges, J.; Schäfer, A. H.; Glorius, F. *Angew. Chem., Int. Ed.* **2010**, *49*, 7786.
(11) Gruttadauria, M.; Giacalone, F.; Noto, R. *Chem. Soc. Rev.* **2008**, *37*, 1666.
(12) Kaur, P.; Hupp, J. T.; Nguyen, S. T. *ACS Catal.* **2011**, *1*, 819.
(13) Mckeown, N. B.; Budd, P. M. *Chem. Soc. Rev.* **2006**, *35*, 675.
(14) Cooper, A. I. *Adv. Mater.* **2009**, *21*, 1291.
(15) Wang, Z.; Chem, G.; Ding, K. L. *Chem. Rev.* **2009**, *109*, 322.
(16) Trewin, A.; Cooper, A. I. *Angew. Chem., Int. Ed.* **2010**, *49*, 1533.
(17) Jiang, J. X.; Su, F. B.; Trewin, A.; Wood, C. D.; Campbell, N. L.; Niu, H. J.; Dickinson, C.; Ganin, A. Y.; Rosseinsky, M. J.; Khimyak, Y. Z.; Cooper, A. I. *Angew. Chem., Int. Ed.* **2007**, *46*, 8574.
(18) Schmidt, J.; Weber, J.; Epping, J. D.; Antonietti, M.; Thomas, A. *Adv. Mater.* **2009**, *21*, 702.
(19) Ben, T.; Ren, H.; Ma, S. Q.; Cao, D.; Lan, J. H.; Jing, X. F.; Wang, W. C.; Xu, J.; Deng, F.; Simmons, J. M.; Qiu, S.; Zhu, G. S. *Angew. Chem., Int. Ed.* **2009**, *48*, 9457.
(20) Chen, L.; Honsho, Y.; Seki, S.; Jiang, D. L. *J. Am. Chem. Soc.* **2010**, *132*, 6742.
(21) Wu, C. D.; Hu, A.; Zhang, L.; Lin, W. B. *J. Am. Chem. Soc.* **2005**, *127*, 8940.
(22) Song, F. J.; Wang, C.; Falkowski, J. M.; Ma, L. Q.; Lin, W. B. *J. Am. Chem. Soc.* **2010**, *132*, 15390.
(23) Ding, S. Y.; Wang, W. *Chem. Soc. Rev.* **2013**, *42*, 548.
(24) Feng, X.; Ding, X. S.; Jiang, D. L. *Chem. Soc. Rev.* **2012**, *41*, 6010.
(25) Ding, S. Y.; Gao, J.; Wang, Q.; Zhang, Y.; Song, W. G.; Su, C. Y.; Wang, W. *J. Am. Chem. Soc.* **2011**, *133*, 19816.
(26) Tanabe, K. K.; Siladke, N. A.; Broderick, E. M.; Kobayashi, T.; Goldston, J. F.; Weston, M. H.; Farha, O. K.; Hupp, J. T.; Pruski, M.; Mader, E. A.; Johnson, M. J. A.; Nguyen, S. T. *Chem. Sci.* **2013**, *4*, 2483.

(27) Shultz, A. M.; Farha, O. K.; Hupp, J. T.; Nguyen, S. T. *Chem. Sci.* **2011**, *2*, 686.

(28) Budd, P. M.; Ghanem, B.; Msayib, K.; Mckeown, N. B.; Tattershall, C. *J. Mater. Chem.* **2003**, *13*, 2721.

(29) Zhang, Y.; Riduan, S. N.; Ying, J. Y. *Chem.—Eur. J.* **2009**, *15*, 1077.

(30) Ma, L. Q.; Wanderley, M. M.; Lin, W. B. *ACS Catal.* **2011**, *1*, 691.

(31) Totten, R. K.; Weston, M. H.; Park, J. K.; Farha, O. K.; Hupp, J. T.; Nguyen, S. T. *ACS Catal.* **2013**, *3*, 1454.

(32) Xie, Z. G.; Wang, C.; DeKrafft, K. E.; Lin, W. B. *J. Am. Chem. Soc.* **2011**, *133*, 2056.

(33) Jiang, J. X.; Wang, C.; Laybourn, A.; Hasell, T.; Clowes, R.; Khimyak, Y. Z.; Xiao, J. L.; Higgins, S. J.; Adams, D. J.; Cooper, A. I. *Angew. Chem., Int. Ed.* **2011**, *50*, 1072.

(34) Chen, L.; Yang, Y.; Jiang, D. L. *J. Am. Chem. Soc.* **2010**, *132*, 9138.

(35) Du, X.; Sun, Y. L.; Tan, B.; Teng, Q. F.; Yao, X. J.; Su, C. Y.; Wang, W. *Chem. Commun.* **2010**, *46*, 970.

(36) Cho, H. C.; Lee, H. S.; Chun, J.; Lee, S. M.; Kim, H. J.; Son, S. U. *Chem. Commun.* **2011**, *47*, 917.

(37) Rose, M.; Notzon, A.; Heitbaum, M.; Nickerl, G.; Paasch, S.; Brunner, E.; Glorius, F.; Kaskel, S. *Chem. Commun.* **2011**, *47*, 4814.

(38) Wang, C. A.; Zhang, Z. K.; Yue, T.; Sun, Y. L.; Wang, L.; Wang, W. D.; Zhang, Y.; Liu, C.; Wang, W. *Chem.—Eur. J.* **2012**, *18*, 6718.

(39) Kang, N.; Park, J. H.; Ko, K. C.; Chun, J.; Kim, E.; Shin, H. W.; Lee, S. M.; Ahn, T. K.; Lee, J. Y.; Son, S. U. *Angew. Chem., Int. Ed.* **2013**, *125*, 6348.

(40) Díez-González, S.; Marion, N.; Nolan, S. P. *Chem. Rev.* **2009**, *109*, 3612.

(41) Samojlowicz, C.; Bieniek, M.; Grela, K. *Chem. Rev.* **2009**, *109*, 3708.

(42) Díez-González, S.; Nolan, S. P. *Aldrichimica Acta* **2008**, *41*, 43.

(43) Jiang, J. X.; Su, F. B.; Trewin, A.; Wood, C. D.; Niu, H. J.; Jones, J. T. A.; Khimyak, Y. Z.; Cooper, A. I. *J. Am. Chem. Soc.* **2008**, *130*, 7710.

(44) Sherrington, D. C. *Chem. Commun.* **1998**, 2275.

(45) Dawson, R.; Laybourn, A.; Khimyak, Y. Z.; Adams, D. J.; Cooper, A. I. *Macromolecules* **2010**, *43*, 8524.

(46) Wang, W. L.; Wu, J. L.; Xia, C. G.; Li, F. W. *Green Chem.* **2011**, *13*, 3440.

(47) Wang, W. L.; Zhang, G. D.; Lang, R.; Xia, C. G.; Li, F. W. *Green Chem.* **2013**, *15*, 635.

(48) Zhu, S. F.; Liang, R. X.; Jiang, H. F. *Tetrahedron* **2012**, *68*, 7949.

(49) Visbal, R.; Laguna, A.; Gimeno, M. C. *Chem. Commun.* **2013**, *49*, 5642.

(50) Collado, A.; Gómez-Suárez, A.; Martin, A. R.; Slawin, A. M. Z.; Nolan, S. P. *Chem. Commun.* **2013**, *49*, 5541.

(51) Galoppini, E.; Gilardi, R. *Chem. Commun.* **1999**, 173.

(52) Simpson, C. D.; Mattersteig, G.; Martin, K.; Gherghel, L.; Bauer, R. E.; Räder, H. J.; Müllen, K. *J. Am. Chem. Soc.* **2004**, *126*, 3139.

(53) Kandambeth, S.; Mallick, A.; Lukose, B.; Mane, M. V.; Heine, T.; Banerjee, R. *J. Am. Chem. Soc.* **2012**, *134*, 19524.

(54) Otera, J. *Modern Carbonyl Chemistry*; Wiley-VCH: Weinheim, Germany, 2000.

(55) Marion, N.; Ramón, R. S.; Nolan, S. P. *J. Am. Chem. Soc.* **2009**, *131*, 448.

(56) Dawson, R.; Laybourn, A.; Clowes, R.; Khimyak, Y. Z.; Adams, D. J.; Cooper, A. I. *Macromolecules* **2009**, *42*, 8809.